surface, interface and nano-structures

EXAFS study of the Fe$_x$/ZrO2 composite nanomaterials obtained by sol-gel synthesis

Vladimir Kriventsov,[a*] **Dmitrii Kochubey,**[a] **Jose Antonio Navio,**[b] **Maria Carmen Hidalgo,**[b] **Gerardo Colón,**[b] **Mark Tsodikov,**[c] **Yuri Maksimov,**[d] **Igor Suzdalev**[d]

[a]*Boreskov Institute of Catalysis, Lavrentyev prosp.,5, Novosibirsk, 630090 , Russia.*
[b]*Instituto de Ciencia de Materiales de Sevilla, Centro Mixto CSIC-Universidad de Sevilla and Dpto. De Quimica Inorganica, Universidad de Sevilla, Avda.Americo Vespucio, 41092-Sevilla, Spain.*
[c]*A.V.Topchiev Institute of Petrochemical Synthesis, 29 Leninskii prosp., Moscow, 117912, Russia.*
[d]*Institute of Chemical Physics, Kosygina st.,4, Moscow, 117977, Russia.*
Email:kriven@inp.nsk.su

The local Zr and Fe arrangements in the nanocomposite system Fe$_x$/ZrO$_2$ (x=0–0.2) obtained by sol-gel method were studied by EXAFS. The phase composition was found to vary significantly on iron loading. For the samples calcined at 500 or 600^{0}C, at x≤0.01, the formed ZrO$_2$ is a mixture of monoclinic and tetragonal structures. Only tetragonal structure is revealed at x≥0.05 with the exception of Fe$_{0.2}$/ZrO$_2$, calcined at 500^{0}C, where new non-typically short Zr-Zr distances (3.29, 3.43Å) were observed. At low iron loading (less than one monolayer) Fe^{3+} ions were found to localize within the pre-surface layers of ZrO$_2$ nanoparticles showing property of isolated ions. For greater Fe loading, iron exhibits either two-dimensional layer structure or two-phase system.

Keywords: zirconia, EXAFS, surface, nanoparticles

1. Introduction

The synthesis of zirconia-based ceramics prepared by sol-gel method from both organic and inorganic precursors makes possible to obtain systems with improved mechanical and electrochemical properties (Shmid et al., 1991; Tsodikov et al., 1995). The structure aspects of mechanism of modification of zirconia-based ceramics by intoduction of a secondary cation are discussed for a long time (Antonioli et al, 1994; Li et al, 1993; Tuilier et al, 1987; Lochman & Tomsia, 1988; Ferenandez et al., 1989; Solier et al., 1993). It has been shown for *4d* (yttrium) and *5f* elements that modification leads either to formation of phase separated (mixed oxide) system or to solid solution where part of Zr^{4+} cations are substituted for modifiers. However, for *3d* elements, the mechanism of modification is still open for discussion. At present two models are thoroughly discussed in the literature. According to the first one, the formation of a mixed oxide prevails. The second model introduces new idea: ion-modifier is not only solved deeply inside ZrO$_2$ structure but also localized on the face of growth. The latter process inhibiting crystal growth may lead to formation of small uniformed nanocrystals and, thus, to formation of ceramics with new unusual properties.

This work deals with the EXAFS study of local Zr and Fe arrangements in the nanocomposite ceramics Fe$_x$/ZrO$_2$ with weight part x varying in the range x=0–0.2. The samples were obtained by sol-gel method.

2. Experiment

2.1. Preparation of samples

ZrO$_2$ and Fe/ZrO$_2$ samples were prepared by hydrolysis of aqueous suspensions of commercial ZrOCl$_2$·8H$_2$O (Merck) containing different amounts of Fe(NO$_3$)$_3$·8H$_2$O (Panreac). Aqueous ammonia (Merck, 25 wt.%) was added drop-wise to the mixture with continuous stirring at pH 9. The digestion time was 3 h. After gelation, the solids were filtered and repeatedly washed in order to be remove chloride ions. In this case the samples showed negative response in AgNO$_3$ test. The gel precursors of the target ceramic were first dried in oven at 100ºC for 24 h, and then calcined either at 500ºC for 24 h or at 600ºC for 3 h with a heating rate of 5ºC/min. The undoped ZrO$_2$ samples were prepared by the same procedure but in the absence of iron.

2.2. EXAFS method

The EXAFS spectra of the Zr-K, Fe-K edges for all samples were obtained at the EXAFS Station of Siberian Synchrotron Radiation Center. The storage ring VEPP-3 with electron beam energy of 2 GeV and an average stored current of 70 mA has been used as the source of radiation. The X-ray energy was monitored with a channel cut Si(111) monochromator. All the spectra were recorded under transmission mode using two ionization chambers as detectors. For the EXAFS measurements, the samples were prepared as pellets with thickness varied to obtain a 0.5-1.0 jump at the Zr-K, Fe-K absorption edges. The EXAFS spectra were treated using the standard procedures (Kochubey, 1992). The background was removed by extrapolating the pre-edge region onto the EXAFS region in the forms of Victoreen's polynomials. Three cubic splines were used to construct the smooth part of the adsorption coefficient. The inflection point of the edge of the X-ray absorption spectrum was used as initial point (k=0) of the EXAFS spectrum. The radial distribution function (RDF) was calculated from the EXAFS spectra in k^{3}χ(k) as modulus of Fourier transform at the wave number interval 4.0-13.2 Å^{-1}.Curve fitting procedure with EXCURV92 (Binsted et al., 1991) code was employed to determine precisely the distances and coordination numbers in similar wave number intervals after
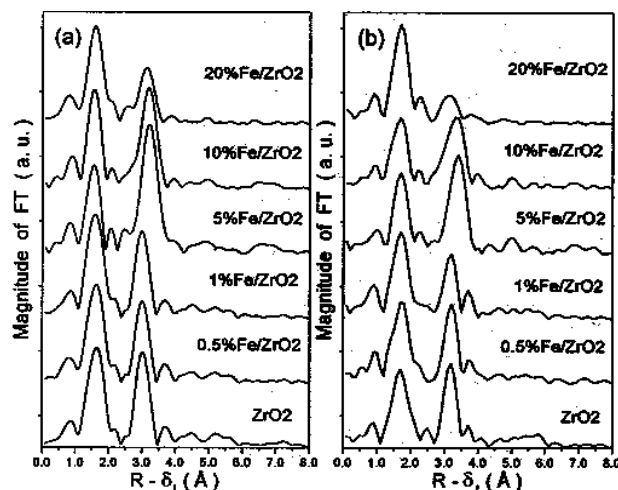
Figure 1

Radial distribution function (RDF) curves describing Zr local arrangement in Fe$_x$/ZrO$_2$ samples calcined at 600^{0}C (a) and 500^{0}C (b).

preliminary Fourier filtering using known XRD data for the bulk Zr and Fe oxides. Debye-Waller factors are fixed (all values are equal to 0.005 Å^2).

3. Results and discussion

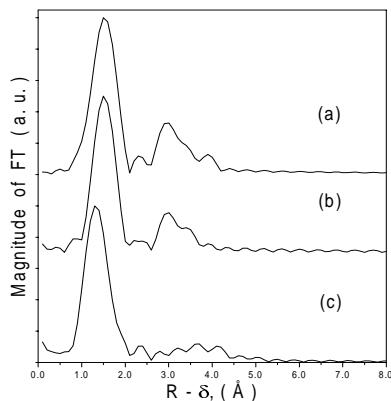For Fe$_x$/ZrO$_2$ samples calcined at 600^{0}C and 500^{0}C, the RDF curves describing local zirconium arrangement are shown in Fig. 1(a, b). The RDF curves of the local iron arrangement for the Fe$_x$/ZrO$_2$ samples calcined at 600^{0}C are shown in Fig.2. For Fe$_x$/ZrO$_2$ ceramics calcined at 600^{0}C and 500^{0}C, The EXAFS data on interatomic distances and coordination numbers describing Zr local arrangement in Fe$_x$/ZrO$_2$ samples calcinated at 600^{0}C and 500^{0}C are presented in Table1. For Fe$_x$/ZrO$_2$ samples calcinated at 600^{0}C the fitting results for two structural models describing Fe local arrangement are summarized in Table 2.

Analysis of the local Zr arrangement in the Fe$_x$/ZrO$_2$ samples, derived from the RDF curves (Fig.1) and EXAFS data (Table 1), allows following conclusions:

1) For the samples calcined at 600^{0}C, at x = 0 – 0.01, ZrO$_2$ is a mixture of monoclinic and tetragonal structures. The increase of x from 0.05 to 0.2 results in only tetragonal ZrO$_2$.

2) For the samples calcined at 500^{0}C, at x = 0 – 0.01, the formed ZrO$_2$ is again a mixture of monoclinic and tetragonal phases while for x = 0.05 – 0.1 only tetragonal structure is typical. However, at x = 0.2 the structure is amorphous that is in a good agreement with the previously obtained data (Navio et al, 2000)).

For tetragonal ZrO$_2$, XRD measurements normally show two Zr-O (2.08, 2.36 Å) and two Zr-Zr distances (3.60, 3.63 Å). It should be emphasized that these values may vary depending on structure distortions. XRD data for monoclinic ZrO$_2$ give seven Zr-O (2.04, 2.06, 2.14, 2.17, 2.20, 2.25, 2.27 Å) and six Zr-Zr distances (3.34, 3.45, 3.46, 3.48, 3.57, 3.93 Å).

As is seen from Table 1, the EXAFS data for undoped ceramics (x = 0) yield only two Zr-O and two Zr-Zr distances. This is in agreement with our structural model in which we used a fixed number of independent parameters. That is why a discrepancy between XRD and EXAFS data is quite reasonable.

Figure 2

RDF curves describing Fe local arrangement in Fe$_x$/ZrO$_2$ samples calcined at 600^{0}C; a) x = 0.2, b) x = 0.1, c) x = 0.05.

Table 1

EXAFS data (distances, coordination numbers) describing Zr local arrangement in Fe$_x$/ZrO$_2$ samples calcined at 600^{0}C and 500^{0}C.

Shell	T-600^{0}C, x						T-500^{0}C, x					
	0	0.005	.01	.05	0.1	0.2	0	0.005	0.01	0.05	0.1	0.2
	R, (N)	R, (N)	R, (N)	R, (N)	R, (N)	R, (N)	R, (N)	R, (N)	R, (N)	R, (N)	R, (N)	R, (N)
Zr-O	2.13 (4.3)	2.12 (4.2)	2.11 (4.5)	2.11 (3.9)	2.10 (4.2)	2.12 (4.4)	2.11 (3.5)	2.10 (3.6)	2.12 (4.0)	2.13 (4.1)	2.12 (3.9)	2.11 (4.9)
Zr-O	2.29 (2.7)	2.28 (2.8)	2.27 (3.1)	2.30 (2.5)	2.28 (2.4)	2.28 (2.9)	2.25 (2.8)	2.25 (2.5)	2.28 (2.5)	2.32 (2.2)	2.29 (2.5)	2.28 (2.7)
Zr-Zr	3.48 (3.4)	3.48 (3.0)	3.46 (2.9)	3.58 (2.9)	3.55 (2.1)	3.52 (1.9)	3.47 (2.3)	3.46 (2.2)	3.48 (2.4)	3.58 (2.3)	3.54 (1.7)	3.29 (0.9)
Zr-Zr	3.65 (1.4)	3.64 (1.4)	3.63 (1.1)	3.65 (1.3)	3.64 (2.1)	3.65 (1.3)	3.65 (0.6)	3.61 (0.6)	3.64 (1.3)	3.67 (1.5)	3.65 (2.4)	3.43 (1.3)
R*	25.1	23.9	24.5	24.1	25.1	23.4	24.7	25.2	25.8	25.1	25.4	25.9

R – distance Zr–O and Zr–Zr, Å
N – effective coordination number
R* – R-factor, %

Our finding that at x ≤ 0.01 and at x ≥ 0.05, two phase (tetragonal and monoclinic) and one phase (tetragonal) system is formed, correspondingly, is in a good agreement with earlier results for a similar zirconia system obtained by XRD (Botta et al, 1999).

The main evidence for formation of monoclinic ZrO$_2$ is the presence of shorter Zr-Zr distance (~3.46Å), while long Zr-Zr distance ~3.6Å retains for x = 0 – 0.01.

The situation with amorphous sample Fe$_{0.2}$/ZrO$_2$ calcined at 500^{0}C is quite different. The Zr-Zr distances (3.29, 3.43Å) do not correspond to any known ZrO$_2$ structures. Earlier Moroz et al, 2000 and Zyuzin et al, 2000 reported on similar short distances (~3.36Å). These distances can be ascribed to a "cubic" ZrO$_2$ structure whose lattice parameter "a" is less than tabular value by 0.3Å. We also observed such unusual distances when studying an aqueous parent solution of zirconium compounds. Thus, we suppose that in this case the initial structure, typical of solution, could be stabilized by anion residues are retained after calcinations.

Analysis of the RDF curves describing local Fe arrangement in the Fe$_x$/ZrO$_2$ (x = 0.05 - 0.2) samples calcined at 600^{0}C (Fig.2) makes possible to suggest isolated Fe ions, deposited on ZrO$_2$ surface. It follows from the fact that peaks corresponding to Fe-Me distances are negligible in Fig.2(c). For x =0.1-0.2 the shift of the most intense peak on the RDF curves to the higher values (Fig.2 a, b) seems to give evidence for formation of sub-oxide and oxide structures. Indeed, at relatively low iron loading (x = 0.05) only single Fe-O peak corresponding to distance ~1.88Å can be seen on the RDF curve (Fig.2c, Table 2). This peak appears to characterize isolated disordered Fe ions deposited on ZrO$_2$ surface. Longer Fe-Fe (Zr) distances (~3.4-3.5Å) can be seen at higher Fe loading (Fig.2a-b, Table 2). The distance ~2.8Å present on the RDF curve is typical for Fe-O-Fe unit in iron oxides (Table 2). However, the corresponding coordination number is less than that for the distance ~3.4Å. This fact makes possible to conclude that Fe ions are mostly deposited on ZrO$_2$ surface forming monolayer while small part of Fe ions is embedded in the second layer. For Fe$_{0.1}$/ZrO$_2$ and Fe$_{0.2}$/ZrO$_2$ samples the presence of Fe-O-Fe distance ~2.8Å may suggest a separate Fe oxide phase formation.

Table 2

EXAFS data (distances, coordination numbers) describing Fe local arrangement in Fe_x/ZrO_2 samples calcined at 600^0C.

Shell		T-600^{0}C, x		
		0.05	0.1	0.2
	R, Å	1.88(1.88)	1.97(1.97)	1.98(1.98)
Fe –O(O)	N	4.5(4.5)	3.1(3.1)	3.6(3.5)
	R, Å	---	2.81(2.85)	2.79(2.80)
Fe-Fe(Fe)	N	---	0.3(0.1)	0.3(0.1)
	R, Å	---	3.49(3.49)	3.51(3.34)
Fe-Fe(Zr)	N	---	0.9(0.8)	1.0(0.9)
R*		24.3(24.8)	16.7(17.8)	22.5(23.6)

R – distance Fe–O and Fe–Fe(Zr), Å
N – effective coordination number
R* – R-factor, %

The question of the structure of such oxide is still open for discussion because fitting procedure gives similar R-factors for both structural models presented in Table 2. In fact, for higher iron loading we can suggest two possibilities. According to the first one the formation of amorphous Fe oxide in addition to isolated Fe ions is quite probable. The second possibility suggests a two-dimensional arrangement with flat Fe-O units associated with the surface of ZrO_2.

Another topic for discussion is the change by ~0.1Å of the Fe-O distance with an increase of Fe loading from x=0.05 to x=0.1 or 0.2. In this case the effective coordination number obtained by EXAFS even decreases. The first distance (~1.88Å) is more typical for Fe tetrahedron arrangement. The second distance (~1.98Å) is more typical for Fe octahedron arrangement. The decrease of the effective coordination number with an increase of Fe-O distance can be treated in terms of increasing distortion around Fe atoms when direct bond Fe-O-Fe (~2.8Å) is formed.

4. Conclusion

The local Zr and Fe arrangements of the composite system Fe_x/ZrO_2 (x=0–0.2) obtained by sol-gel synthesis were studied by EXAFS. The new non-typical short Zr-Zr distances (3.29, 3.43Å) are observed in the sample $Fe_{0.2}/ZrO_2$ (500^0C). It was found out that in all cases Fe ions are deposited on the surface of ZrO_2 nanoparticles forming either isolated ions at the concentrations less than one monolayer or/and two-dimensional layer structure or iron oxide phase at higher iron loading.

5. References

Antonioli G., Lottici P.P., Manzini I., Gnappi G., Montenero A., Paloschi F., Parent P. (1994) J. Non.Cryst. Solids. **177**, 179-186.

Binsted, N., Campbell, J.V., Gurman, S.J. & Stephenson, P.C. (1991*). EXCURV92 program*, SERC Daresbury Laboratory, UK.

Botta, S.G., Navio, J.A., Hidalgo, M.C., Restrepo, Litter, M.I. (1999). *J. Photochem. Photobiol. A: Chem.* **129**, 89-99

Ferenandez, R.Z.D., Hammon, A. & Hammoucke, A. (1989). *Solid State Ionics.* **37**, 31

Kochubey, D.I. (1992). *EXAFS spectroscopy of catalysts*, edited by D.I. Kochubey, pp. 5-99. Novosibirsk: Nauka.

Li, P., Chen, I.W., Pennerhahn, J.E. (1993). *Phys. Rev. B* **48**(14), 10074-10081.

Lochman, R.E. & Tomsia, A.P.(1988). *Am.Seram.Soc.Bull.* **67**, 375

Moroz, E.M., Ivanova, A.S., Ziouzin, D.A. (2000). *J. Mol. Cat. A: Chem.* **158**, 313-317

Navio, J.A., Macias, M., Sanches-Soto, P.J., Hidalgo, M.C., Restrepo, G.M., Botta, S.G., Litter, M.I., Tsodikov, M.V. (2000). In preparation.

Shmid, R., H. Ahamandan, H. & A. Mosset, A. (1991). *Inorg. Chim. Acta.* **190**, 237

Solier, J.D., Cachadina, I., Domingez-Rodriguez, A. (1993). *Phys.Rev.* **48**(6), 3704

Tsodikov, M.V., Bukhtenko, O.V., Ellert, O.G., Shcherbakov, V.M, Kochubey, D.I. (1995). *Mater. Sci.* **30**, 1087

Tuilier, M. H., Dexpert-Ghys, J., Dexpert, H., Lagarde, P. (1987). *J. Solid State Chem.* **69**(1), 153-161.

Zyuzin, D.A., Moroz, E.M., Ivanova, A.S. & Zaykovskii, V.I. (2000). *Inorg. Materials* **36**(4), 447-451